

Performance Evaluation of Direct Vessel Injection Plus (DVI+)

Tae-Soon Kwon*.

*Author for correspondence

Korea Atomic Energy Research Institute, P.O.Box 105, Yuseong, Daejeon, 305-600, Rep. of KOREA,

E-mail: tskwon@kaeri.re.kr

ABSTRACT

A new advanced safety feature of DVI+(Direct Vessel Injection Plus) for the APR⁺ (Advanced Power Reactor plus), to mitigate and to prevent an ECC(Emergency Core Cooling) bypass phenomena, is presented for an advanced DVI system(DVI+). A protective ECC flow down channel from a high-speed cross flow in a downcomer, a 4-duct which is called an ECC extension duct is installed on the outside of a core barrel. In this study, the feasibility of DVI+ has been tested. They include: (1) 1/5-Scale air-water test, (2) DVI+ duct vibration test, (3) full scale duct injection test. The other design verification tests are also performed. They include: (1) Full scale 3-Fuel assembly cross flow test, (2)1/5-Scale reactor flow distribution test (to be performed, under construction), (3) Core simulator calibration developing test for core flow test. The duct vibration test and the ECC intake fraction tests are performed using full scale DVI duct test facility. The ECC bypass fraction is measured under the condition of the steady-state and direct ECC bypass. The water level of reactor downcomer is controlled at a lower level to prevent the sweep out phenomena from the free surface of collapsed water. A CFD (Computational Fluid Dynamics) analysis was also performed for the simplified scaled model using commercial CFD code. The test results show that the ECC direct bypass fraction is much reduced when the DVI+ duct is applied. The DVI+ ECC extension duct is a good feature to mitigate and to prevent the ECC direct bypass.

INTRODUCTION

An ECC direct bypass depends on the geometrical configuration of the DVI nozzle and its location in the downcomer (T.S. Kwon et al., 2003, H. Glaeser, 1992, 1993). The entrainment of ECC water in a downcomer is strongly dependent on the relative azimuthal angle between the broken cold leg and the ECC injection nozzle. Therefore, this azimuthal angle effects induce a different ECC bypass characteristics versus the number of ECC injection nozzle. In some case, the ECC bypass fraction of 4-EDG (Emergency Diesel Generator) system would be increased when compared

to that case of 2-EDG system. The new DVI+ Emergency Core Cooling System (ECCS) is different from the current DVI system which are applied to the APR1400, AP1000, or US-APWR combined injection system, which uses both a DVI and Cold Leg Injection (CLI) system. In an advanced pressurized water reactor APR+, a DVI extension duct which is installed on an outer surface of core barrel is newly applied into the downcomer annulus to prevent strong steam-water interaction in the reactor downcomer during a postulated loss of coolant accident. The major design goal of the DVI+ system is to mitigate the direct ECC bypass for a 4-EDG (T.S. Kwon et al., 2003). The relative azimuthal injection angle of a DVI nozzle is defined as the angle from the broken cold leg to the hot leg. The current DVI azimuthal injection angle of APR1400 is 15 degrees. A high relative azimuthal angle gives a low ECC bypass fraction in general (T.S. Kwon et al., 2003, 2004).

SEPARATE EFFECT TESTS

ECC BYPASS PERFORMANCE TEST FOR DVI+ DUCT

The direct ECC bypass and sweep out behavior in the reactor downcomer annulus is strongly dependent on the Wallis parameter. Because the downcomer gap of the APR+ is reduced by the ECC duct in the downcomer annulus, the circumferential steam velocity is increased when compared to that of the APR1400. However, the developing test of DVI+ is performed on the 1/5-Scale air-water test facility DIVA for the APR1400. Therefore, to evaluate the ECC bypass behavior for the APR+ based on the 1/5-scale DIVA air water test results, the Wallis parameters for each plant is compared. The increased Wallis parameter for APR+ drives the ECC bypass increasing though the geometrical conditions such as the downcomer gap and its height, pipe diameter of hot leg and cold leg, and the break size are not changed except the core power increased by 7% in the APR+. However, the ECC bypass fraction of the APR+ does not increase because the DVI+ duct prevents the steam-water interaction in the downcomer annulus. In this scaling parameter comparison, the

dimensionless circumferential velocity $j_{g,ent}^*$ and $j_{l,ent}^*$ are compared by equation(1).

$$\begin{aligned} (j_{g,eff}^*)_R &= \frac{\left(\frac{\dot{M}_{g,eff}}{\rho_g \cdot A_{Flow}} \left[\frac{\rho_g}{(\rho_f - \rho_g) \cdot g \cdot L_{DC}} \right]^{1/2} \right)_{APR+}}{\left(\frac{\dot{M}_{g,eff}}{\rho_g \cdot A_{Flow}} \left[\frac{\rho_g}{(\rho_f - \rho_g) \cdot g \cdot L_{DC}} \right]^{1/2} \right)_{APR1400}} \quad (1) \\ &= (\dot{M}_{g,eff})_R * \frac{1}{(Gap_{D/C})_R} = 1.07 * \left(\frac{1}{0.8} \right) \\ &= 1.3375 \end{aligned}$$

where,

$$\begin{aligned} (\dot{M}_{g,eff})_R &= \frac{(CoreSteamFlow)_{APR+}}{(CoreSteamFlow)_{APR1400}} = 1.07 \\ (L_{DC})_R &= \frac{(D_{CL})_{APR+}}{(D_{CL})_{APR1400}} = 1 \\ (A_{Flow})_R &= \frac{(L_{D/C} * Gap_{D/C})_{APR+}}{(L_{D/C} * Gap_{D/C})_{APR1400}} \\ &= \frac{(Gap_{D/C})_{APR+}}{(Gap_{D/C})_{APR1400}} \\ &= \frac{20}{25} = 0.8 \end{aligned}$$

and, the subscripts

g gas phase
 f fluid
 CL cold leg
 D/C downcomer

The DVI nozzle and ECC extension duct are designed to open without any mechanical connections. A pipe connector is completely removed from between each direct vessel injection nozzle and each injection extension duct installed on an outer surface of the core barrel, which are opposite to each other. An emergency core cooling water intake port, through which the water is injected from each direct vessel injection nozzle, is formed on the surface of each injection extension duct facing an axis of each direct vessel injection nozzle. Thereby, the emergency core cooling water is injected into the intake hole of the ECC extension duct from the direct vessel injection nozzle by a hydraulic flow momentum.

The injection extension duct, which protrudes from the core barrel toward the reactor vessel, preferably has a radial distance limited to a range less than 1/5 of the downcomer gap. This is because, in the case in which the radial distance must be smaller than the minimum inner diameter of the upper

alignment key portion of the reactor vessel and the inner diameter of the hog leg. No interference occurs when the reactor vessel and the core barrel are assembled or when the neutron monitoring capsule is withdrawn.

As shown in Fig. 1, the lowest outlet of the ECC extension duct is designed to be open, and the highest cap of the ECC extension duct is closed, and it includes at least one air vent so that gas can be discharged when the nuclear reactor vessel is filled with water. The ECC water intake port is located on the axial line of the DVI nozzles. The diameter of the emergency core cooling water intake port is about one to two times of the inner diameter of the DVI nozzle in consideration of a deflection of the jet by means of gravity when the jet of the DVI nozzle has small spreading and flow rates. Thereby, the emergency core cooling water is can be entered more easily into the ECC extension duct.

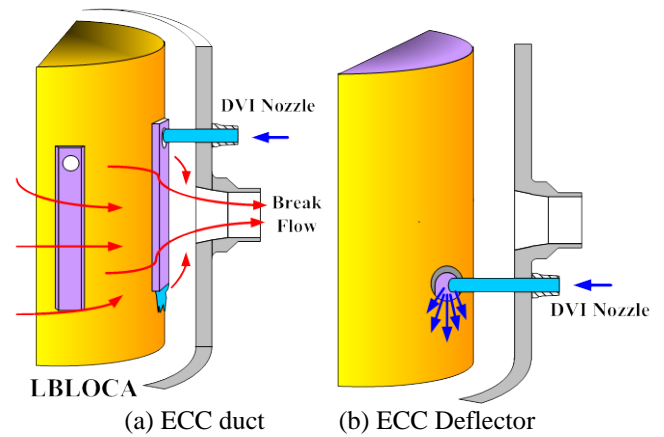


Fig. 1 ECC duct installation location

AIR-WATER ECC BYPASS TEST CONDITIONS

To evaluate the ECC bypass performance of the ECC duct and the ECC deflector systems, the air-water 1/5-scale reactor downcomer model of the APR1400 is applied. The test loop has 4 cold legs, 2 hot legs blunt body, and 4 DVI nozzles. The reference plant is the APR1400 which is 2-loop pressurized light water reactor. The RCS of the APR1400 consists of 2 hot legs and 4 cold legs. The DVI water injection velocity is fixed at 0.72 m/sec. The air velocities of 3 cold legs are varied from 5 m/sec to 20 m/sec. The water level of the downcomer was controlled at low level.

AIR-WATER ECC BYPASS TEST RESULTS

The ECC direct bypass fractions with injection nozzle variation are compared in Fig.2. The black solid squared symbol represents the DVI-2 and DVI-4 combination for the 1/5-scale air-water model of the original APR1400 without the DVI+ duct. The total bypass fraction is about 42% at a velocity of 20 m/sec. The ECC direct bypass fraction hits about 68% for

the combination of the DVI-1 and DVI-4 of 4-EDG system at the cold leg velocity of 18 m/sec. The ECC direct bypass is strongly mitigated when compared to the combination of the DVI-1 and DVI-4 injection. The results for the DVI+ duct system show that the ECC bypass performance of the 4-EDG system is lower than that of the 2-EDG system when the single failure assumption and the maintenance concept are applied at the same time during LOCA.

Fig. 3 represents the performance of the ECC deflector system. The ECC deflector has the role of an ECC momentum directional controller. The direct bypass fraction of the ECC extension duct is about 10% for the velocity range of 0~15 m/s. while the ECC bypass fraction is increasing very sharply over 50~60 %.

In figures, the ECC bypass performance between the ECC deflector and the DVI+ duct are compared. As shown in figures, the ECC bypass fraction of the ECC deflector is higher than that of the DVI+ duct in the velocity range of 15~20 m/s .

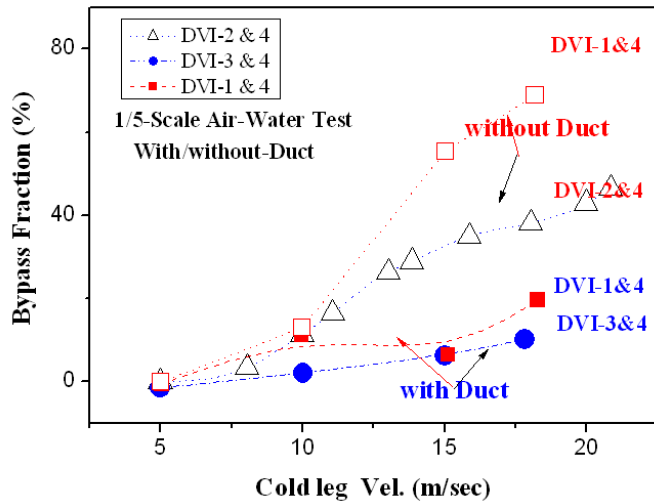


Fig. 2 Comparison of ECC Bypass fraction

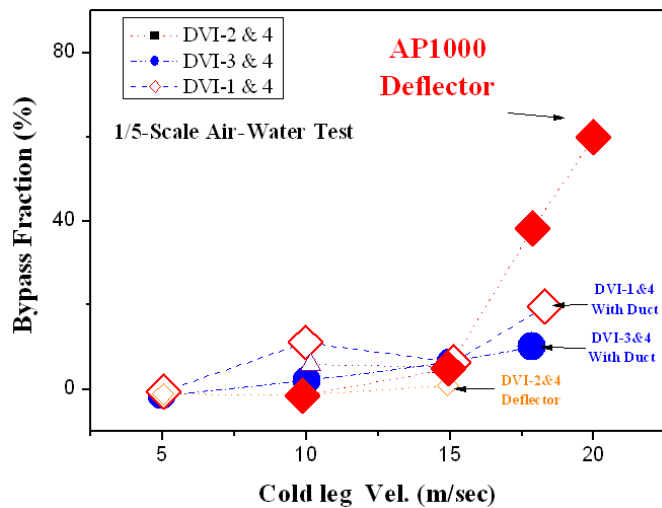


Fig. 3 ECC Bypass of ECC Deflector

VIBRATION TEST

In this study, the modal tests and analyses for two types of duct surfaces have been carried out as shown in Fig. 4. Since the DVI duct has a thin shell of 5 mm thickness, so that the harmonic responses of the RCP blade pressure perturbation of 240 Hz should be checked. The dominant passing frequencies are known to be 120, 240, and 480 Hz. The natural frequencies of the full scale duct in a few low modes were obtained by a numerical simulation and modal test. The fundamental modes coincide within the narrow band except that of the arch duct under water; the numerical simulation gave 50.2 Hz while the modal test yielded 38.9 Hz. The Fig. 5 shows the frequency response of duct in the water. The Fig. 6 shows the low frequency modes of the arch duct in air by CFD.

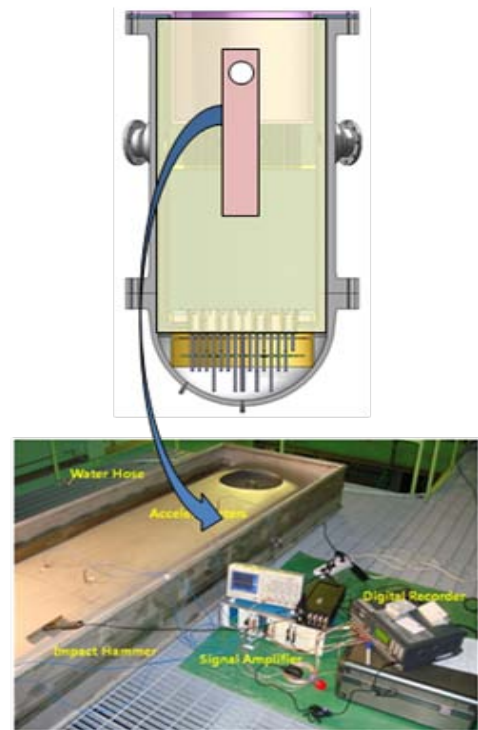


Fig. 4 Vibration test of the full scale duct

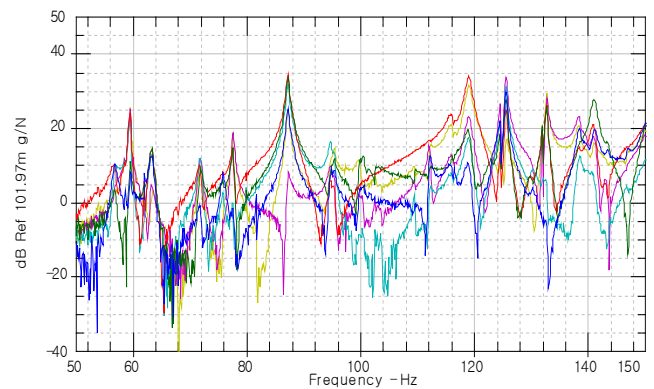


Fig. 5 Frequency response of duct (in water)

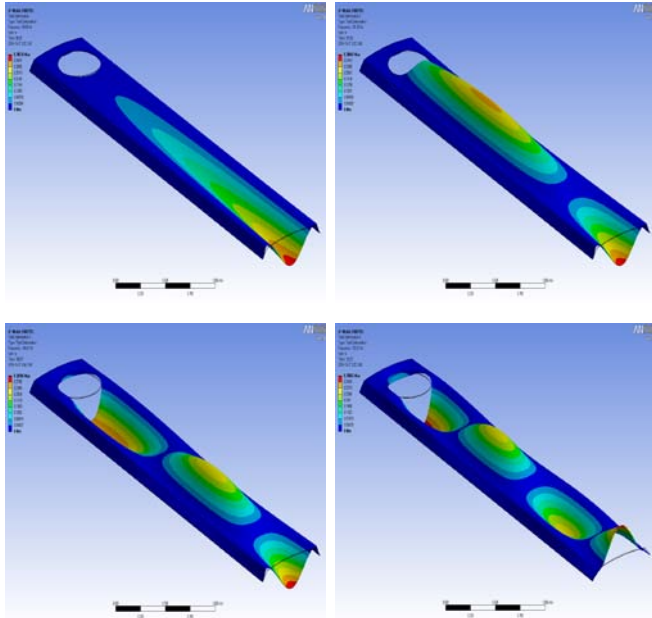


Fig. 6 Four low modes of the arch duct in air

Table 1 Scaling ratio

Parameter	Scale ratio
Velocity ratio, v_R	1/1
Mass Injection Ratio, m_R	1/1
Downcomer gap, $Gap_{R,Duct}$	1/1
Duct Width, W_R	1/1
Duct Height, H_R	1/1

Table 2: ECC water spillage fraction

ECC Duct intake shape	Average Injection Velocity (m/s)	Spillage Fraction (%)
Elliptical	1.792	12.102
	1.641	5.886
	1.566	4.770
Circular	1.757	4.013
	1.584	3.181

FULL SCALE DUCT ECC SPILLAGE TEST

The test was performed at the conditions of atmospheric pressure and room temperature. The circular shaped intake duct geometry leads lower spillage fraction than that of the elliptical shaped intake duct. The scaling parameters are summarized in Table 1. The Fig. 7 shows the schematics of test facility.

The ECC water spillage fraction is defined by Eq. (2).

$$\text{ECC spillage fraction (\%)} = \frac{m_{spill}}{m_{in}} \times 100 \quad (2)$$

where, m_{in} was the integrated injected mass of the ECC water, and m_{spill} was the integrated spillage mass.

The spillage fraction is about 3~4% for the shape of circular intake hole. The spillage ratio is summarized in Table 2. Fig. 8 shows an ECC flow pattern for the circular shaped intake. The ECC water spillage fraction increased with the ECC water injection velocity, in case the circular shaped intake duct had a lower spillage fraction than that of the elliptical shaped intake duct. The reflection of the ECC water at the core barrel surface was increased when the ECC injection velocity was increased. This phenomenon increased the ECC spillage fraction. In the case of the circular shaped intake duct, the ECC spillage fraction was reduced due to the minimized water reflection from the duct when compared with an elliptical shaped intake duct.

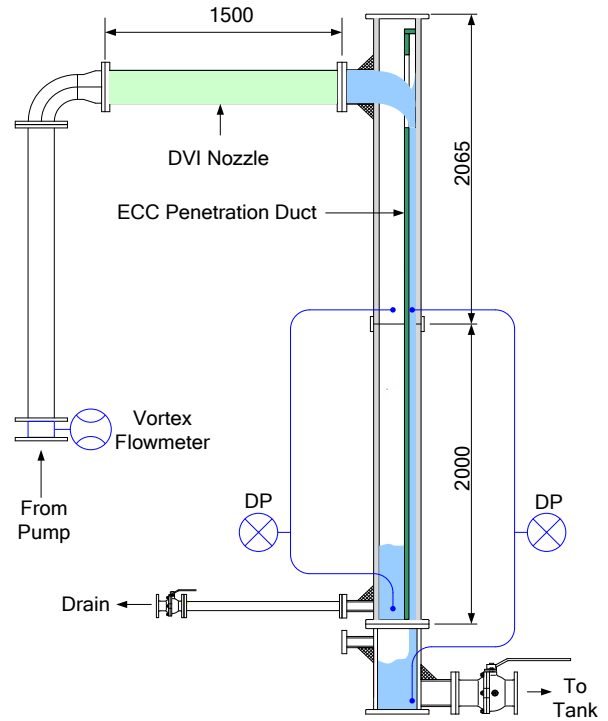


Fig. 7 Full scale duct spillage test facility

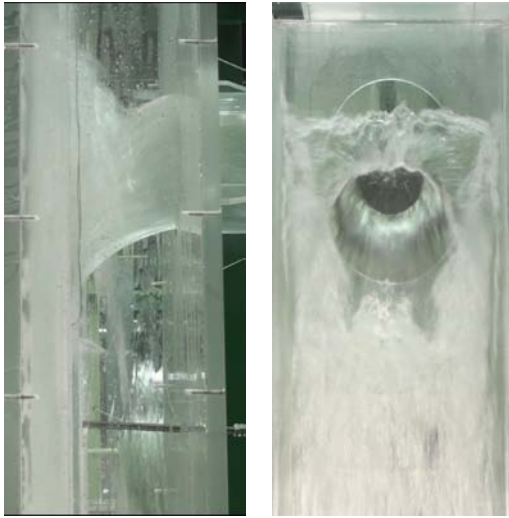
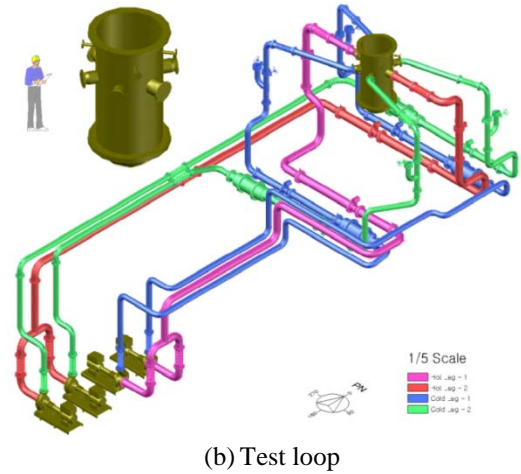


Fig. 8 ECC flow patterns ($v_{in} = 1.58$ m/s).

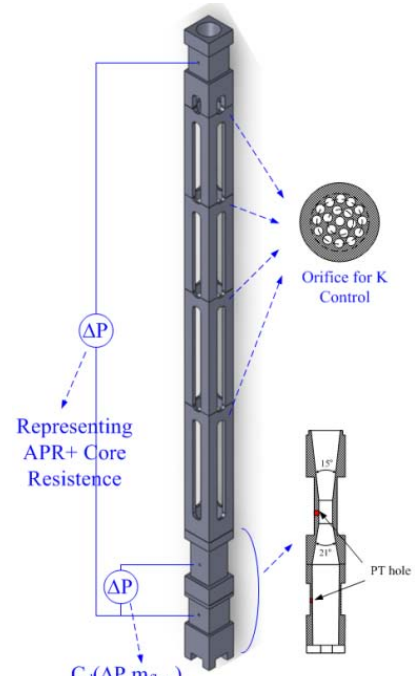


(b) Test loop

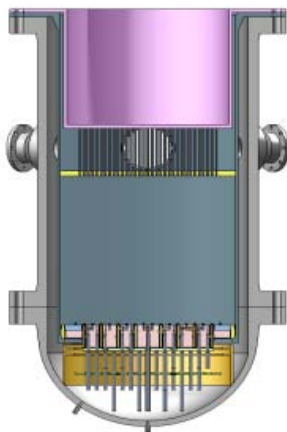
Fig. 9 ACOP test facility

ACOP CORE FLOW TESTS

The APR+ has a 257-F/A core configuration. To evaluate the core thermal margin, the core flow and pressure distribution data are needed. For this purpose, the reactor flow test facility was designed based on the conservation of Euler number, which is a ratio of pressure drop to dynamic pressure with a sufficiently high turbulent region. The ACOP test facility is designed linearly reduced to a 1/5 ratio with a 1/2 velocity scale, which yields a 1/39.7 Reynolds number scaling ratio. Fig.9 shows the overall configuration of the ACOP test facility. Fig.10 shows the overall configuration of the core simulator. All the core simulators are calibrated to have a relationship between mass flowrate and pressure drop. Fig. 11 shows the cross flow characteristics of the core simulator are evaluated by CFD simulation. The flow differences between adjacent F/A are $\pm 10\%$. The axial flow differences are disappeared with the channel cross flow. The general cross flow characteristics are coincided well.



(a) Core Simulator configuration



(a) 1/5-scale reactor vessel



(b) 257-Core simulator assembly

Fig.10 Core Assembly

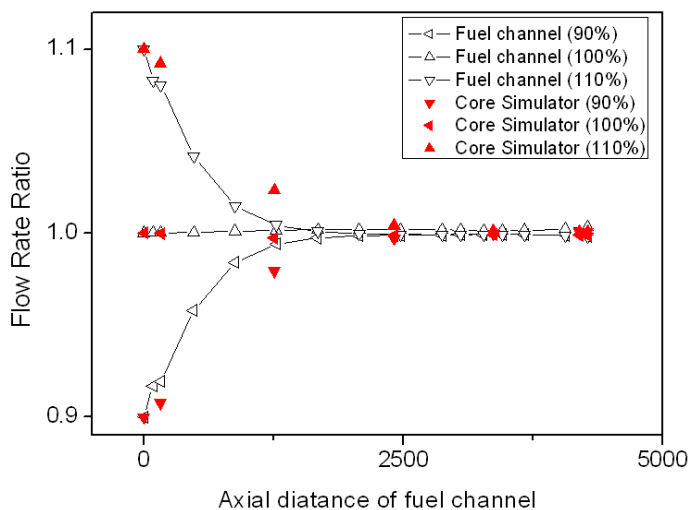


Fig.11 Cross flow characteristics

CONCLUSIONS

The current status of the thermal-hydraulics R&Ds for APR+ at KAERI were reported, which is being performed in very close conjunction with the standard design verification and developments. The main R&D issues related with thermal hydraulic performance tests of DVI+ and core flow tests using core simulator for the APR+ reactor are briefly introduced. The commercial CFD code is also applied to verify the model similarity for the flow characteristics of core flow and the vibration characteristics of DVI+. The numerical test results were applied for the development of preliminary test models. The new safety concepts of APR+ will be fully verified in terms of their performance and applicability to the safety system enhancement. The core flow test using ACOP test facility will be performed by the end of year 2012.

ACKNOWLEDGMENTS

This research has been performed as a part of the nuclear R&D program supported by the Ministry of Knowledge Economy of the Korean government.

REFERENCES

[1] Bae, B.U., "Development of CFD Code for Subcooled Boiling Two-Phase Flow with Modeling of the Interfacial Area Transport Equation," Ph.D. Thesis, Seoul National Univ., 2008.

[2] T. S. Kwon, C. R. Choi, and C.-H. Song, "Three-dimensional analysis of flow characteristics on the reactor vessel downcomer during the late reflood phase of a

postulated LBLOCA", Nuclear Engineering and Design (NED), Vol. 226, pp.255-265(2003).

[3] T. S. Kwon, C.-H. Song, B. J. Yun, and H. K. Cho, "Effect of the Yaw Injection Angle on the ECC Bypass in Comparison with the Horizontal DVI", Nuclear Engineering and Design (NED), 225, pp.295-304(2003).

[4] H. Glaeser, "Downcomer and tie plate countercurrent flow in the Upper Plenum Test Facility(UPTF)", Nuclear Engineering and Design, 133, 259-283 (1992).

[5] H. Glaeser and H. Karwat, "The contribution of UPTF experiments to resolve some scale-up uncertainties in countercurrent two phase flow", Nuclear Engineering and Design, 145, 63-84 (1993).

[6] T. S. Kwon, Y.S. Shin, S.H. Hwang, C.H. Song., "Effect of Azimuthal Injection Angle on the ECC direct bypass in a DVI System", KNS, 2004 Autumn.

[7] T. S. Kwon, Y.S. Shin, S.H. Hwang, C.H. Song., "Proposal of a Dual Core Barrel for New Safety Injection Concept", KNS, 2004 Autumn.

[8] T. S. Kwon, Y.S. Shin, S.H. Hwang, C.H. Song, "Effect of Water Column Type of DVI Injection on the Direct ECC Bypass", KNS, 2004 Autumn

[9] T.S. Kwon et al, "Advanced DVI for ECC Direct Bypass Mitigation", Nuclear Engineering and Design (NED) Available online 9 March, 2009.

[10] D.J. Euh et al., "Development of a Test Facility to Simulate the Reactor Flow Distribution of APR+", the Korean Nuclear Society Spring Meeting Taebaek, Korea, May 26-27, 2011

[11] Heung Seok KANG et al., "MODAL ANALYSIS OF AN ECC DUCT FOR APR+ REACTOR BARREL", The 14th International Topical Meeting on Nuclear Reactor Thermal Hydraulics (NURETH-14).

[12] Seungtae Lee "Experimental Study of ECC Duct Bypass for Development of an Advanced DVI+", Transactions of the Korean Nuclear Society Spring Meeting Pyeong Chang, Republic of Korea, May 27~28, 2010.

[13] B. U. Bae et al., "Experimental Study on Cooling Performance of Condensation Heat Exchanger in PAFS (Passive Auxiliary Feedwater System)", The Fifth China-Korea Workshop on Nuclear Reactor Thermal Hydraulics (WORTH-5), Chengdu, China, October 10~12, 2011.

[14] W. P. Baek et al., "KAERI Integral Effect Test Program and the ATLAS Design", Nuclear Technology, Vol. 152, No. 183, 2005.

[15] A. N. Nahavandi et al., "Scaling Laws for Modeling Nuclear Reactor Systems", Nucl. Sci. & Eng., Vol. 72, pp. 75~83, 1979.